SUBBAND ADAPTIVE REGULARIZATION METHOD FOR REMOVING BLOCKING EFFECT

Sung-Wai Hong *Yuk-Hee Chan* *Wan-Chi Siu*

Department of Electronic Engineering,
The Hong Kong Polytechnic University,
Hong Kong

ABSTRACT

This paper presents two new approaches to remove blocking effect in low-bit rate transform coded images by using subband decomposition/reconstruction technique. They are designed to act as a supplementary post-processing step of the JPEG standard. Both approaches make use of the noise characteristic of each subband to bound the maximum tolerable error and the smoothness of the restored images in restoring subband images with regularization. One of them will also utilize the spatial activity of the restoring images to tighten the bounds. Computer simulations showed that the new adaptive objective functions could achieve a better restoration performance in terms of both subjective and objective measures than did other conventional objective functions.

1. INTRODUCTION

Discrete cosine transform (DCT) coding is a well established technique for image compression and has been adopted as the basic compression algorithm in the JPEG standard. In DCT compression, image is first divided into small non-overlapping blocks (usually 8×8 or 16×16) and each block is transformed with a 2-dimensional (2-D) DCT. Then, high-frequency (HF) coefficients of the transformed blocks are discarded, and the remaining low-frequency (LF) coefficients are quantized. However, block-based transform coding results in "blocking effect" [1, 2] at high-compression ratio. The blocking effect leads to the perception of visible discontinuity between adjacent blocks. In this paper, we present a spatially non-adaptive and a spatially adaptive subband approaches to remove this annoying artifact in the reconstructed images. These approaches are fully compatible with the JPEG standard.

2. REGULARIZATION APPROACH

A linear space-invariant image degradation system can be modeled as

$$y = Bf + n, \tag{1}$$

where vectors y ,f and n (lexicographically ordered by either column or row, from the size of $N \times N$ into $N^2 \times 1$) are the degraded image, the original image and the additive noise, respectively. Matrix B is the linear distortion operator of size $N^2 \times N^2$, and y would be the blocky image that we reconstructed. In our case, B represents an operation which consists of the block DCT compression, quantization and decompression.

Regularization [6, 7] is an effective technique to convert an ill-posed problem to a well-posed one. Yang, Galatsanos, and Katsaggelos proposed an objective function (CLS1) [1] for tackling the blocking effect. In particular, the objective function is defined as :

$$J_{\alpha_1} = \alpha_1 \|Sf\|^2 + \|y - f\|^2, \tag{2}$$

where S is a regularizing operator of dimension $N^2 \times N^2$, which is generally a high-pass filter used to reduce the amount of noise (usually in the form of HF) in the restored image. $\| \bullet \|$ represents the Euclidean norm. Let ϵ_1^2 and ϵ_2^2 be the bounds for $\|y - f\|^2$ and $\|Sf\|^2$, respectively, i.e., $\|y-f\|^2 \leq \epsilon_1^2$, and $\|Sf\|^2 \leq \epsilon_2^2$. The former bound is for the error that we can tolerate. With this constraint only, the solution obtained is an inverse filter which will amplify the noise during the restoration. Hence, satisfying the former constraint may have a side effect of noise amplification. The latter bound imposes a smoothness upperbound and suppresses the HF content of the whole image by means of the regularizing operator. The principle of regularization is to find the best estimate that compromises these two constraints. The ratio α_1 $(= \frac{\epsilon_1^2}{\epsilon_2^2})$ is the regularization parameter that controls the degree of smoothness of the resulting image.

A solution to the fore-mentioned problem can be obtained by minimizing the objective function (eqn.(2)) with respect to f. The iterative method, which has a number of advantages [8], is given by

$$f(k+1) = f(k) + \beta_1 (y - (I + \alpha_1 S^t S) f(k)), \tag{3}$$

where I is the identity matrix and X^t denotes the transpose of matrix X. The relaxation parameter β_1 is a scalar, which has to be within the range $0 < \beta_1 < \frac{2}{\|I + \alpha_1 S^t S\|}$ to ensure the convergence of the iteration. The iteration $f(k)$ will converge to a unique estimate of the original image.

This work was supported by The Hong Kong Polytechnic University Grant A/C No. 350.255.A3.420

0-8186-7310-9/95 $4.00 © 1995 IEEE

3. PROBLEM FORMULATION IN SUBBAND DOMAIN

The basic technique of subband decomposition and reconstruction [3] can be briefly explained as follows: The input image is decomposed into several narrow bands by passing through an analysis filter bank. Subband images are then sub-sampled for further processing. In reconstruction, processed subbands are up-sampled and filtered for interpolation with a synthesis filter bank. Then they are recombined to form the reconstructed image. It is desirable to design the analysis/synthesis filter banks [3] in such a way that they can remove aliasing between subbands and achieve perfect reconstruction.

For alias-free subband decomposition, the degradation model in subband domain [4, 5] becomes

$$y_i = B_i f_i + n_i \qquad \text{for i} = 1, \ldots, \text{M}. \quad (4)$$

where y_i, B_i, f_i, and n_i are the sub-sampled observed image, the subband distortion operator, the original image, and the noise respectively of the ith subband. M is the number of decomposed subbands.

Figure 1 depicts four subband images of a JPEG encoded image (0.26 bit/pixel). The image is decomposed with an 8-tap perfect reconstruction-quadrature mirror filters (PR-QMFs) [3]. Subband LL is very close to the JPEG encoded version. Subbands LH, HL and HH contain the horizontal, vertical and diagonal features of the original JPEG encoded image, respectively. The appearance of the horizontal and vertical line segments in subbands LH and HL are caused by the quantization process of the independent block-based transform coding scheme. It is obvious that, better images could be achieved by adapting the restoration models to the characteristic of each subband separately. In other words, we aim at adapting the regularization technique to the appearance of the blocking artifact of each subband.

4. SPATIALLY NON-ADAPTIVE SUBBAND APPROACH

We propose the following new subband objective functions for a M-subband approach :

$$J^s_{\alpha_2} = \alpha^s_2 \|W^s_L S^s f^s\|^2 + \|W^s_R (y^s - f^s)\|^2, \quad (5)$$

where $s \in M$ subbands. In these functions, W^s_L and W^s_R are diagonal weighted matrices of dimension $\frac{N^2}{M} \times \frac{N^2}{M}$. Parameter α^s_2, S^s, f^s and y^s are defined as before for a particular subband. There exists a trade off between computational load and the number of subbands. We have found that a 4-subband system is robust enough for this application, with an acceptable increase in computational load only. For a 4-subband system, we have $s \in \Lambda \equiv$ { LL, LH, HL, HH }.

In highly compressed JPEG encoded natural images, most HF DCT coefficients are discarded. Therefore, in subband domain, the low-frequency subband (subband LL) will contain relatively large amount of signal energy than the mid-frequency (subbands LH and HL) and high-frequency subbands (subband HH). Usually, subband HH almost contains no signal energy. Hence, for subband HH, where the signal-to-noise ratio (SNR) is the lowest, noise suppression should have an overwhelming effect. Subbands LH and HL are with moderate SNRs, and characterized by the blocking artifact, which is apparently observed as horizontal or vertical lines segments. Therefore, noise suppression should be specifically strengthened in these segments, while moderate restoration condition is applied to other regions. As most of the signal energy is retained in subband LL, similar restoration conditions should be applied as in the fullband image.

Based on the above arguments, we adjust parameters W^s_L and W^s_R for particular subband. To simplify the weighted matrices determination, subband LL is taken as the reference for determining the weighted matrices for the other subbands. Hence, we have $W^{LL}_L = W^{LL}_R = I$. For subband HH, we have $W^{HH}_R = 0I$ and $W^{HH}_L = \gamma I$, where $\gamma \geq 1$, to remove the HF component amplification effect and enhance the noise suppression effect simultaneously. Similarly, for subbands LH and HL, where noise suppression strength can be approximated to be that in subband HH, we have $W^{LH}_L = W^{HL}_L = W^{HH}_L$. As for W^{LH}_R and W^{HL}_R, they should be determined according to their noise characteristics as follows :

$$W^{LH}_R(i,i) \text{ or } W^{HL}_R(i,i) = \begin{cases} 0 & \text{if it is coincides with the line segments,} \\ \mu & \text{otherwise,} \end{cases} \quad \text{for i} = 1, \ldots, \tfrac{N^2}{4}.$$

where μ is a scalar weight, with the range $0 < \mu < 1$. Hence, we can rewrite eqn.(5) as :

$$J^{LL}_{\alpha_2} = \alpha_2 \|S^{LL} f^{LL}\|^2 + \|y^{LL} - f^{LL}\|^2, \quad (6)$$

$$J^{LH}_{\alpha_2} = \gamma\alpha_2 \|S^{LH} f^{LH}\|^2 + \|W^{LH}_R (y^{LH} - f^{LH})\|^2, \quad (7)$$

$$J^{HL}_{\alpha_2} = \gamma\alpha_2 \|S^{HL} f^{HL}\|^2 + \|W^{HL}_R (y^{HL} - f^{HL})\|^2, \quad (8)$$

$$J^{HH}_{\alpha_2} = \gamma\alpha_2 \|S^{HH} f^{HH}\|^2. \quad (9)$$

Instead of looking for a solution which minimizes all four objective functions with respect to their corresponding subband images simultaneously, we minimize a linear combination of the above equations with respect to the fullband image. In formulation, we have

$$\frac{\partial J_{\alpha_2}}{\partial f_{fullband}} = \frac{\partial (J^{LL}_{\alpha_2} + J^{LH}_{\alpha_2} + J^{HL}_{\alpha_2} + J^{HH}_{\alpha_2})}{\partial f_{fullband}} = 0. \quad (10)$$

Since it is very difficult to determine an optimal regularization operator (S^s) for each subband, an alternative objective function (SCLS1) given as

$$J_{\alpha_3} = \alpha_3 \|S \sum_{s \in \Lambda}^{\Re} [W^s_L f^s]\|^2 + \|\sum_{s \in \Lambda}^{\Re} [W^s_R (y^s - f^s)]\|^2 \quad (11)$$

is exploited instead, where $\sum_{s \in \Lambda}^{\Re} [\bullet]$ is the reconstruction operator which combines all four subbands to reconstruct an image with the synthesis filter bank. For each iteration, instead of performing regularization to each subband separately, the subbands predicted and the prediction error of each subband are respectively weighted by their specific W^s_L and W^s_R first. Then, the weighted terms are reconstructed into fullband domain before SCLS1 is performed.

Function SCLS1 is spatially non-adaptive as it is based on the linear space-invariant image model (eqn.(1)). Since

this model may simplify the nature of natural images, performing SCLS1 on spatial varying images may not get a good result. In this case, modification of SCLS1 is necessary to preserve the high spatial activity components (e.g. edges) of the restoring images.

5. SPATIALLY ADAPTIVE SUBBAND APPROACH

In order to restore the sharpness of the restored images, a new spatial adaptive subband function (SCLS2) that embeds the spatial activity information of the restoring images is presented. This function is defined as

$$J_{\alpha_4} = \alpha_4 \| LS \sum_{s \in \Lambda}^{\Re} [W_L^s f^s] \|^2 + \| R \sum_{s \in \Lambda}^{\Re} [W_R^s (y^s - f^s)] \|^2, \quad (12)$$

where R and L are both diagonal weighted matrices and defined as in [2], so as to compromise the effect of the constraints with respect to the spatial activity [2]. Minimizing the objective function (12) with respect to f results in the following iterative equation :

$$f(k+1) = f(k) + \beta_4 (R^t R y - (R^t R + \alpha_4 S^t L^t L S) f(k)). \quad (13)$$

6. SIMULATION RESULTS

In our computer simulations, three typical 256-level test images, 'Baboon', 'Lena' and 'Hat' were selected. They are all of size 256×256. The spatial activity distribution of these images range from high to low [9]. The test images were divided into 8×8 blocks and transform-coded with JPEG scheme to generate blocky images. The blocky images were then restored by making use of CLS1 (eqn.(2)), as well as our proposed SCLS1 (eqn.(11)) and SCLS2 (eqn.(12)), with initial estimates prepared by using the approach proposed in [2].

A 3×3 Laplacian filter was used as the regularization operator S. The regularization parameters were chosen to be $\alpha_1 = (\frac{\epsilon_1}{\epsilon_2})^2$ and $\alpha_3 = \alpha_4 \simeq 4\alpha_1$. 8-tap PR-QMFs, which are designed to minimize the interband aliasing energy of the filtered signals [3], were used as the analysis/synthesis filter banks. The PPSNR was used as an objective criterion of merit. Criterion $\frac{\|f_k - f_{k-1}\|^2}{\|f_k\|^2} \leq 2 \times 10^{-10}$ was used to terminate the iterative processes. The PPSNR is defined as

$$10\ log_{10} \frac{(255)^2}{\sum_{i=1}^{256} \sum_{j=1}^{256} (g_{i,j} - x_{i,j})^2} \quad \text{dB}, \quad (14)$$

where $g_{i,j}$ and $x_{i,j}$ are the (i,j)th pixels of the original and the output images respectively.

Table 1 lists the PPSNR improvements (IPPSNR) of the restored images and the number of iterations required to achieve these performance. It is obvious that our proposed functions yield better objective measures than CLS1 does. On the average, the objective improvement of our proposed functions are approximately 3.4 times over that of CLS1 in terms of dB. It is easy to realize that, SCLS2 yields the best objective measures among the three functions, for all test images.

Figure 2 shows the magnified portion of a JPEG encoded 'Lena' (PPSNR = 28.3573 dB). Figure 3, 4 and 5 are the magnified portions of 'Lena' after being processed by CLS1, SCLS1 and SCLS2 respectively. With our proposed objective functions, the restored images are free from the blocking effect. Especially with SCLS2, the sharpness of the restored images is well restored and preserved.

7. CONCLUSIONS

In this paper, we presented two new adaptive objective functions for the constrained least square regularization approach to remove the blocking artifact. Findings reveal that the proposed objective functions performed better than the regularization approach proposed in [1], on both objective and subjective measures.

8. REFERENCES

[1] Y. Yang, N. P. Galatsanos and A. K. Katsaggelos, "Regularized reconstruction to reduce blocking artifacts of block discrete cosine transform compressed images," *IEEE Trans. on Circuits and Systems for Video Technology*, Vol. 3, No. 6, pp. 421-432, Dec. 1993.

[2] S. W. Hong, Y. H. Chan and W. C. Siu, "An adaptive constrained least square approach for removing blocking effect," *IEEE International Symposium on Circuits and Systems*, Vol. 2, April. 1995.

[3] A. N. Akansu and R. A. Haddad, *Multiresolution signal decomposition: transforms, subbands, and wavelets*, Academic Press, Inc..

[4] N. P. Galatsanos and R. T. Chin, "Digital restoration of multichannel image," *IEEE Trans. on Acoustics, Speech, and Signal Processing*, Vol. 37, No. 3, pp. 415-421, Mar. 1989.

[5] M. R. Banham, N. P. Galatsanos, H. L. Gonzalez and A. K. Katsaggelos, "Multichannel restoration of single channel images using a wavelet-based subband decomposition," *IEEE Trans. on Image Processing*, Vol. 3, No. 6, pp. 821-833, Nov. 1994.

[6] K. Stewart and T. S. Durrani, "Constrained signal reconstruction - a unified approach," *EURASIP Signal Processing III*, pp. 1423-1426, 1986.

[7] A. K. Katsaggelos and R. M. Mersereau, "A regularized iterative image restoration algorithm," *IEEE Trans. on Signal Processing*, Vol. 39, No. 4, pp. 914-929, Apr. 1991.

[8] A. K. Katsaggelos "Iterative image restoration algorithms," *Optical Engineering*, Vol. 28, No. 7, pp. 735-748, July 1989.

[9] V. R. Algazi, Y. Kato, M. Miyahara and Kotani, "Comparison of image coding techniques with a picture quality scale," *Proc. SPIE Applications of Digital Image Processing XV*, Vol. 1771, pp. 396-405, 1992.

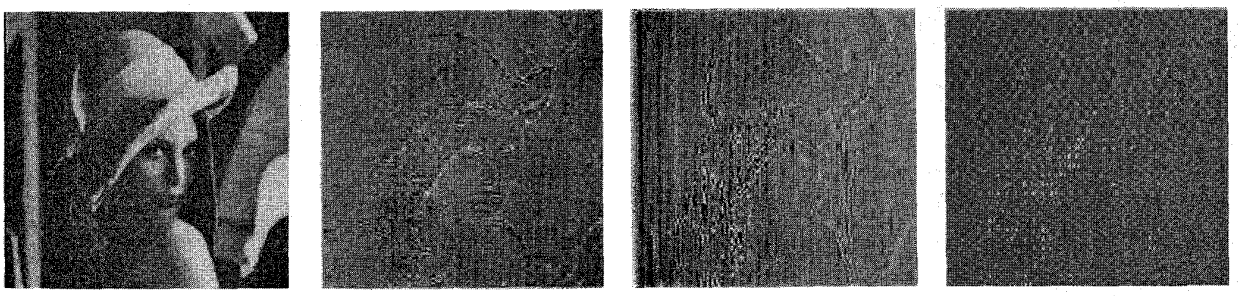

a: subband LL
size: $\frac{N}{2} \times \frac{N}{2}$

b: subband LH
size: $\frac{N}{2} \times \frac{N}{2}$

c: subband HL
size: $\frac{N}{2} \times \frac{N}{2}$

d: subband HH
size: $\frac{N}{2} \times \frac{N}{2}$

Figure 1: Four subbands of a JPEG encoded image.

Table 1: The experimental results for the test images.

JPEG encoded image	bit/pixel	IPPSNR (# of iterations)		
		CLS1 [1]	SCLS1	SCLS2
'Baboon'	0.33	0.084dB(13)	0.146dB(04)	0.151dB(08)
'Lena'	0.26	0.136dB(13)	0.490dB(07)	0.541dB(19)
'Hat'	0.28	0.210dB(14)	0.994dB(20)	1.037dB(20)

Figure 2: JPEG encoded 'Lena'.

Figure 3: CLS1 processed 'Lena'.

Figure 4: SCLS1 processed 'Lena'.

Figure 5: SCLS2 processed 'Lena'.